PERGAMON

Journal of Structural Geology 23 (2001) 941–950

JOURNAL OF STRUCTURAL GEOLOGY

www.elsevier.nl/locate/jstrugeo

Weakening associated with the diaspore–corundum dehydration reaction in metabauxites: an example from Naxos (Greece)

Janos L. Urai[a,*], Anne Feenstra[b]

[a]*Lithosphere Dynamics Group, RWTH Aachen, Lochnerstrasse 4-20, Aachen, Germany*
[b]*GeoForschungsZentrum Potsdam, Experimental Petrology/Geochemistry, Telegrafenberg, D-14473 Potsdam, Germany*

Received 12 January 1999; accepted 5 April 2000

Abstract

Metabauxite lenses embedded in marble on Naxos consist of diasporites below the 420°C isograd, and dehydrate into corundum-rich rocks with increasing grades of metamorphism. While the diasporites are essentially undeformed, the corundum-rich rocks are strongly deformed, even though both diasporites and corundum-rich rocks are much stronger than the surrounding intensely deformed marbles. The observed structures can be explained as an effect of high fluid pressures during the prograde diaspore–corundum dehydration reaction, which causes dramatic temporary weakening of the metabauxites (to a strength comparable to that of the surrounding deforming marbles). Deformation of the metabauxite is thus largely restricted to the time span the phase transformation occurred, allowing the dehydrating bauxite mass to deform together with the surrounding marbles.

1. Introduction

The mechanical properties of rocks undergoing prograde metamorphism are not well understood. Study of field examples is difficult due to the complex interplay of chemical reactions and deformation mechanisms, often involving transient microstructures which are not preserved in the final rock fabric.

The key processes involved are:

1. Generation of low effective pressures by rapid production of high pressure fluids. This process is illustrated in the classic undrained deformation experiments of Raleigh and Paterson (1965) on serpentinite and Heard and Rubey (1966) on gypsum. Here the water generated by dehydration reactions was unable to leave the system and developed the high pore pressures necessary to activate fracturing in the samples. This drop in effective pressure leads to dramatic weakening and associated dilatancy. In nature this process is more complex and mechanical properties are strongly dependent on the competition between rates of fluid production, the evolution of porosity and permeability, and the rate of removal of fluid from the reaction site. Recent experimental and theoretical work by Olgaard et al. (1994), Ko et al. (1995, 1997) and Wong et al. (1997) has shown the conditions under which the dehydration process can lead to excess pore pressures, resulting in weakening and embrittlement of the reacting mass.
2. The initial reaction products can be very fine-grained (depending on nucleation and growth kinetics), before they coarsen into the final microstructures. Fine grain size, combined with the presence of a pore fluid (even at less than lithostatic pressures) can lead to a switch in deformation mechanism to diffusional creep processes (Rutter and Brodie, 1988; Newman et al., 1999), which are strongly grainsize sensitive and can lead to dramatic weakening.
3. Phase transformations or changes in environmental conditions (Paterson and Luan, 1990), e.g. changes in f_{H_2O} or f_{O_2}, which may lead to enhancement of intracrystalline creep processes.

In this paper we describe observations which point to a transient, dramatic weakening during prograde metamorphism of metabauxite units embedded in deforming marbles on the island of Naxos. The weakening is inferred to occur during the transformation of diasporite into emery, involving the reaction

$$2\ \text{diaspore}\ (\alpha\text{-AlOOH}) = \text{corundum}\ (\alpha\text{-}Al_2O_3) + \text{water}\ (H_2O)$$

* Corresponding author.
E-mail addresses: j.urai@ged.rwth-aachen.de (J.L. Urai), feenstra@gfz-potsdam.de (A. Feenstra).

0191-8141/01/$ - see front matter
PII: S0191-8141(00)00165-6

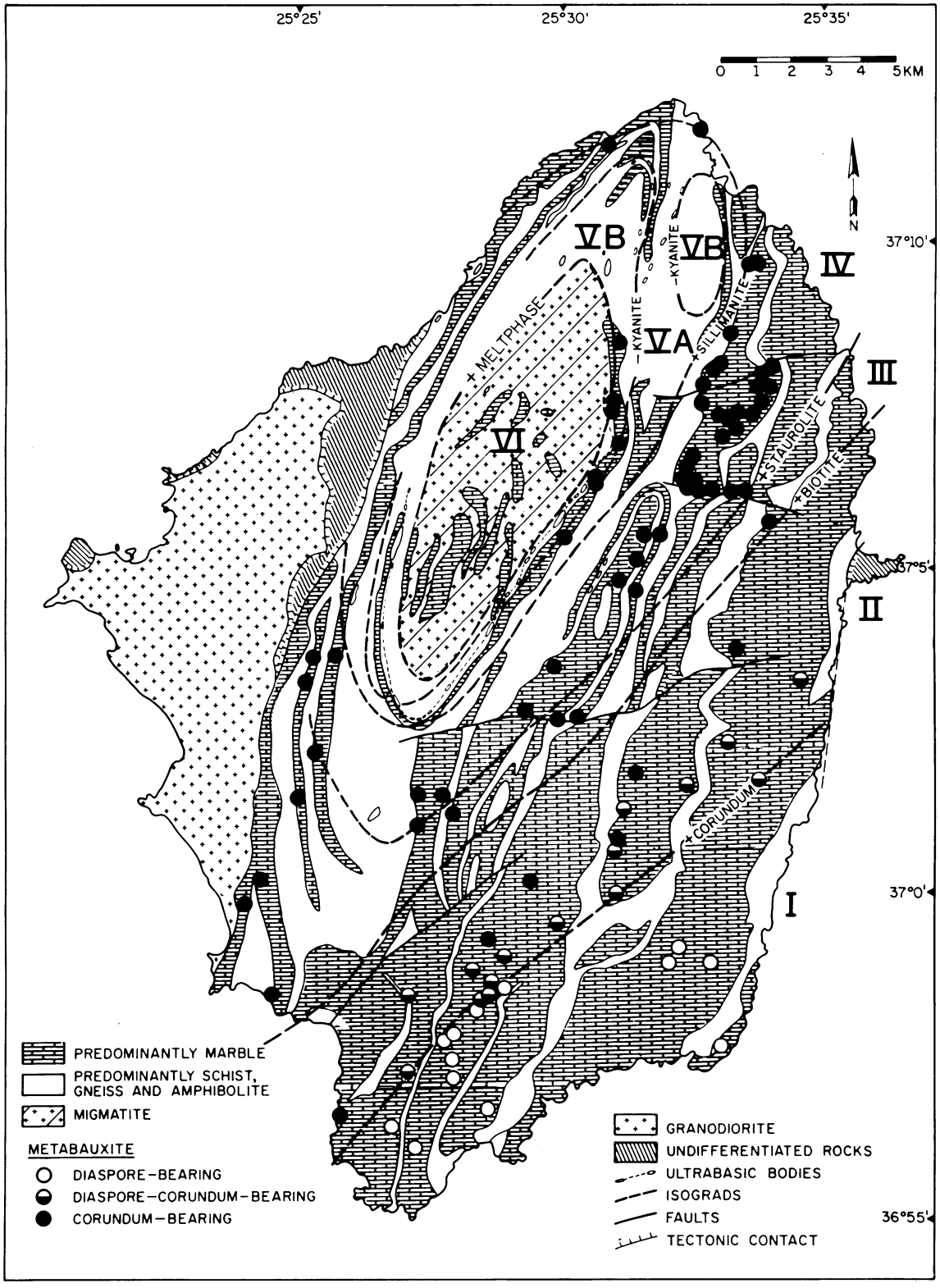

Fig. 1. Geological map of Naxos showing the main rock types, isograds, metamorphic zones (I–VI) and metabauxite occurrences (after Feenstra, 1985). The following isograds were mapped with increasing M2 grade: corundum-in (~420°C, in metabauxites); biotite-in (~500°C, in metapelites); Fe-rich staurolite-in (~540°C, in metabauxites and metapelites); sillimanite-in (~620°C, in metapelites); kyanite-out (~650°, in metapelites); meltphase-in (~670°C, in metapelites).

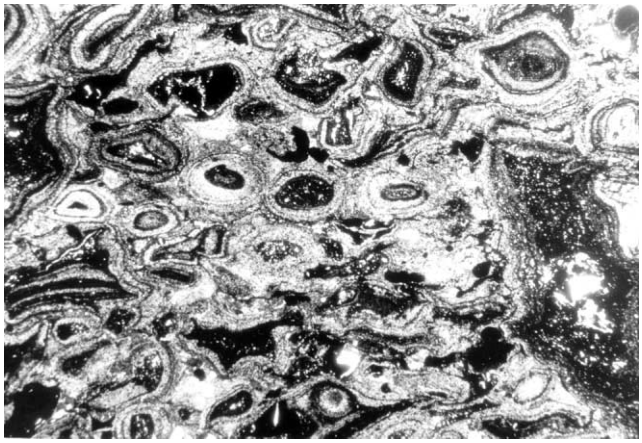

Fig. 2. Photomicrograph of an essentially undeformed diasporite from zone I. The pisoids consist of concentric shells of diaspore and hematite. Sample AFN28, plane polarized light, width of photo is 10 mm.

The preliminary work reported here concentrated on the samples described by Feenstra (1985), who studied the mineralogy, petrology and geochemistry of the Naxos metabauxites. Unfortunately, only a few of these samples were sectioned along the principal axes of finite strain (thin sections were cut perpendicular to foliation if discernible). Full quantitative analysis of strain was therefore not possible, and the data presented here only give approximate information on the finite strain in the samples. Further detailed work on additional samples is in progress.

2. Geological setting

The rocks on Naxos belong to the Attic–Cycladic Metamorphic Belt (Jansen and Schuiling, 1976; Ridley, 1982; Lister et al., 1984; Andriessen et al., 1987; Wybrans and McDougall, 1988; Okrusch and Bröcker, 1990; Andriessen, 1991; Gautier et al., 1993; Gautier and Brun, 1994). Marbles

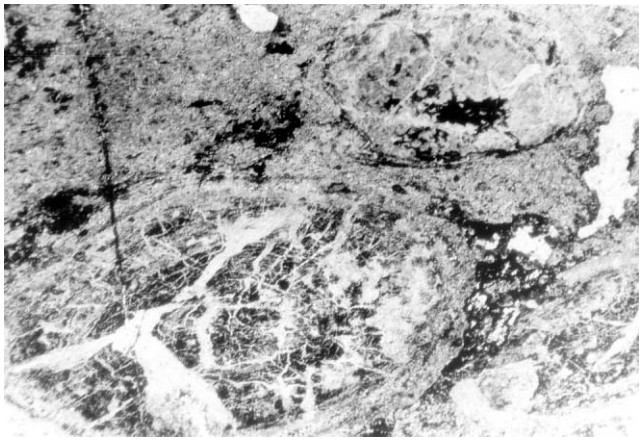

Fig. 3. Photomicrograph of a weakly deformed diasporite from zone I. Pisoids are cut by frequent early veins. Sample AF122B, plane polarized light, width of photo is 25 mm.

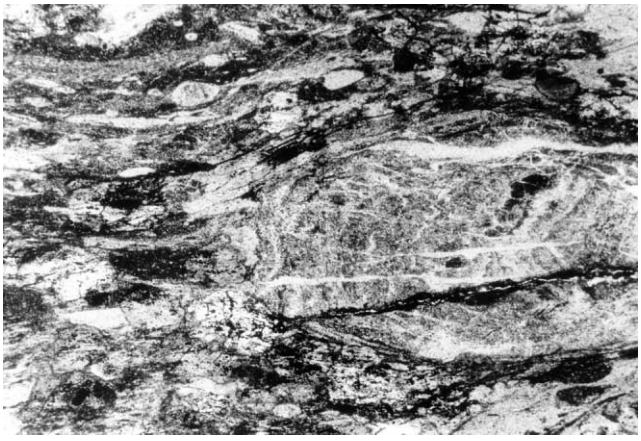

Fig. 4. Photomicrograph of a weakly deformed diasporite from zone I, very close to the corundum-in isograd. Pisoids are cut by small veins and show the first signs of ductile deformation (this thin section does not contain corundum but other samples from nearby outcrops contain 1–5% corundum). Sample AF32C, plane polarized light, width of photo is 10 mm.

of Mesozoic age and various types of schists, gneisses and metavolcanics (Mesozoic to upper Paleozoic in age) are the dominant rock types.

The history of the Attic–Cycladic Metamorphic Belt comprises an early Alpine compressional tectonic phase (ending between 40–50 Ma), which involved subduction of continental margin material, generation of a nappe pile and regional high-pressure (P), low-temperature (T) metamorphism (M1), followed by a regional greenschist facies overprint (M2) at 20–25 Ma.

The onset of extensional tectonics in Early Miocene, probably triggered by southward retreat of the N-dipping subduction zone south of Crete (Spakman et al., 1988; Lister and Baldwin, 1993), resulted in the formation of a back-arc basin with a thinned crust, high heat flow, intrusion of granitoid magmas (Pe-Piper et al., 1997), and localized high-T medium-P metamorphism (M2: Jansen and Schuiling, 1976; Buick and Holland, 1989).

3. Geological evolution of Naxos

The rocks of the Naxos core complex (Fig. 1) can be divided into four distinct units:

1. an Alpine metamorphic complex consisting of interbedded marbles, schists, gneisses;
2. a migmatite complex;
3. a 13 Ma granodiorite; and
4. an upper tectonic unit of allochthonous, non-metamorphic rocks.

The metamorphic complex consists of metacarbonates, pelites, amphibolites, quartzites, metavolcanics and metagranitic rocks. Minor rock types include metamorphosed karstbauxites and ultramafics. The allochthonous upper

(a)

(b)

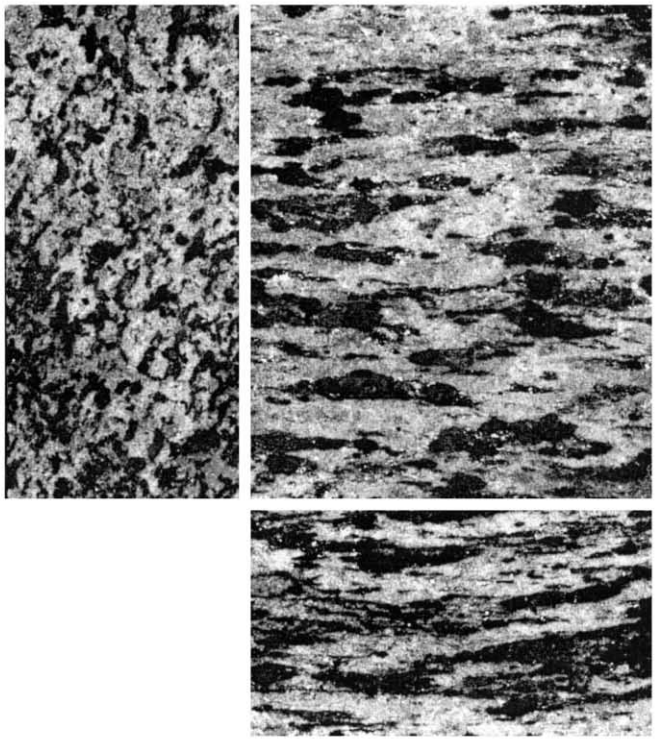

(c)

plate unit above the Naxos detachment fault is exposed in Eastern and in Western Naxos (Fig. 1; Lister and Forster, 1998); where it overlies the granodiorite, the upper plate is unaffected by contact-metamorphism (Jansen and Schuiling, 1976).

The effect of the Eocene high-pressure metamorphism (M1) is preserved in the rocks of Southeastern Naxos, where partly overprinted blueschist facies assemblages are found. Here mineral assemblages point to M1-temperatures of 400–460°C at minimum pressures of 0.7–0.9 GPa (Feenstra, 1985). The high-grade M2 event took place between 20 and 16 Ma, and resulted in peak temperatures between ~700°C in the migmatite dome and ~400°C in Southeastern Naxos at pressures of ~0.6 GPa (Jansen and Schuiling, 1976; Feenstra, 1985; Wybrans and McDougall, 1988; Buick and Holland, 1989; Andriessen, 1991; Baker and Matthews, 1995; Lewis et al., 1998). The six isograds which have been mapped in pelitic and bauxitic rocks divide the complex into seven metamorphic zones (Fig. 1).

The metamorphic complex consists of a strongly deformed sequence, containing kilometre-scale isoclinal folds with fold axes trending N–S, coaxially refolded by open, upright folds (Hecht, 1979; Urai et al., 1991). This regional fabric forms a structural dome with the foliation warping over the migmatite complex. There is a penetrative foliation and a well-developed stretching lineation in most units. Deformed calcitic pebbles commonly show aspect ratios of ~1:6:30 with the long axis parallel to the regional lineation, reflecting strain accumulated during M1 and M2. All field structures support the presence of a major crustal shear zone in the metamorphic complex, active during the M2 metamorphism, reworking rocks strongly deformed during M1.

The high-grade M2 fabric is locally overprinted by late, narrow shear zones formed during cooling (Buick, 1991a, b). Sense of shear is consistently 'upper plate moving north' for all syn- and post-M2 deformation (Urai et al., 1991). Rapid uplift of lower crustal rocks was completed on Naxos about 5 Ma ago along a low angle, crustal scale shear zone-detachment fault system (Boronkay and Doutsos, 1994; John and Howard, 1995; Morris and Anderson, 1996).

4. The metabauxites

4.1. Geology and petrology

Metabauxites are found enclosed in marbles in all metamorphic zones, except zone VI. Most deposits are part of discontinuous stratigraphic horizons that can be followed along strike over distances of several kilometres, although isolated occurrences are also found. It is likely that there were initially 2–3 different stratigraphic bauxite horizons, which have been repeated by large-scale isoclinal folding and thrusting (Bonneau et al., 1978; Hecht, 1979). Geochemical studies of trace element distributions along vertical profiles across metabauxite lenses indicate that the metabauxites are partly in an overturned position (Feenstra, 1985).

Mineralogically the metabauxites can be divided into two types: diasporites and emeries. Dehydration of the former into corundum-dominated rocks (corundites) is smeared out over a 1–2 km wide zone, in which primary diaspore and corundum coexist in the deposits (Fig. 1).

Metabauxites in zone I are mostly fine-grained rocks without discernible foliation, containing diaspore–hematite–chloritoid–rutile with minor amounts of calcite, muscovite and paragonite. The diasporites are relatively small (0.5–4 m thick) angular bodies intercalated in strongly deformed marbles.

Many diasporites display the subspherical pisoidic–ooidic textures commonly found in non-metamorphic karstbauxites, which are considered to be of syn- to diagenetic origin (Bardossy, 1982). The Naxos pisoids are typically between 0.1 and 10 mm in diameter and usually consist of alternating shells of diaspore and hematite (Fig. 2). More rarely chloritoid-rich layers are present in the pisoids. In most cases the pisoids in the diasporites are not visibly distorted, although they can be non-spherical. Some pisoids are cross-cut by late veinlets filled with diaspore and less commonly with white mica (Figs. 3 and 4).

The first appearance of corundum, typically found in the outer rims of the metabauxite lenses, has been mapped as the corundum-in isograd (Feenstra, 1985, see Fig. 1). Textural and petrographical features observed in the transition zone (Feenstra, 1985) involve epitaxial intergrowths of corundum and diaspore, suggesting the stable coexistence of both phases, and the presence of 1–10 mm wide veinlets filled with corundum and minor calcite. Contrary to the corundum in the matrix, which is crowded with inclusions of hematite and rutile, the vein corundum is commonly free of solid inclusions.

Metabauxites northwest of the diaspore–corundum transistion are emeries. In zones II and III the emeries are characterized by the assemblage corundum–chloritoid–hematite–rutile and in zone IV by corundum–staurolite–biotite–kyanite–magnetite–ilmenite. Prograde margarite, the dominant mica in the emeries, first appears in the transition zone and remains stable until the upper part of

Fig. 5. (a) Photograph of the region between two commercial (mined out) emery boudins, with a smaller body in the boudin-neck. Note the foliation in the surrounding marbles curving around the boudins. E–W section, photograph taken looking south in zone IV. (b) Photograph of three sides of an emery sample from zone IV cut parallel and perpendicular to the foliation. Light grey regions are rich in corundum, dark regions in Fe–Ti-oxides. Short side of sample is 3 cm. (c) Photograph of a polished slab of an emery sample from zone IV showing ductile folding. Light grey bands are rich in corundum and silicates, darker bands in corundum and Fe–Ti-oxides. Width of picture is 15 cm.

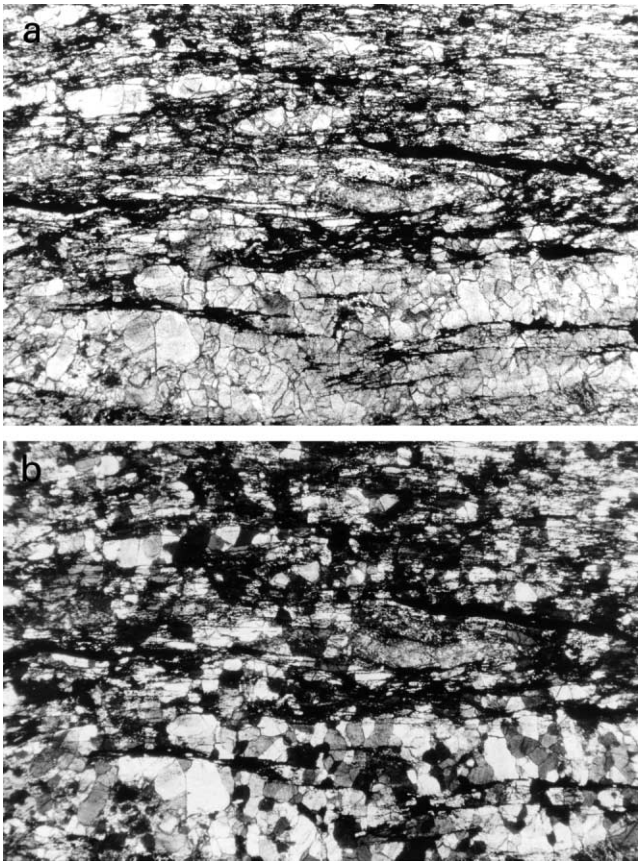

Fig. 6. Photomicrograph of an emery sample from zone IV, with strongly deformed pisoids and the formation of a foliation defined by Fe–Ti oxides. This fabric is overgrown by corundum. Sample N05A, width of photo is 25 mm. (a) Plane polarized light; (b) crossed polarizers.

zone IV, where it dehydrates to anorthite plus corundum (Feenstra, 1996).

Upgrade of the corundum-in isograd, the metabauxites show an increasing amount of deformation (Fig. 4). Most of the emeries occur in N–S elongated boudins [Fig. 5(a)]. They typically are 3–5 m thick (sometimes reaching a thickness of 10 m) and usually are much larger than the diasporite bodies in zone I. Many emeries of zones III and IV show a strong internal foliation and lineation [Fig. 5(b)], always parallel to the long axis of deformed pisoids. In a number of cases, banded emeries containing up to several millimetre-thick corundum layers are folded in a fully ductile fashion [Fig. 5(c)]. Pisoids, where present, are usually strongly deformed with aspect ratios up to 1:30 (Fig. 6). In the samples which were oriented, the long axis of deformed pisoids was parallel to the regional stretching lineation in the surrounding marbles.

Microstructures in the emeries indicate ductile deformation of varying homogeneity, with the original fine Fe-rich bands strongly deformed and bent around thicker, flattened but undisrupted Al-rich parts of the pisoids. These deformation structures are in turn overgrown by undeformed corundum porphyroblasts (grain size 0.05–0.8 mm) with well-developed foam textures (Fig. 6). In addition, typical amphibolite-facies minerals (zone IV and V) such as staurolite, biotite and anorthite are randomly oriented. Corundum shows a clear tendency to increase in grain size with increasing M2 grade, reaching a maximum grain size of 0.6–1.0 mm in zone VB near the migmatite. The latter emeries lack pisoidic and banded structures and show a granoblastic texture defined by corundum and magnetite–ilmenite grains, suggesting advanced high-T recrystallization under static conditions. Table 1 summarizes the microstructural observations made in this study. The thin sections described in this table were not oriented, so that the axial ratios of the pisoids cannot be used for quantitative strain determination. Nevertheless, the data show a clear relationship between the diaspore–corundum transformation and the onset of deformation and development of foliation in the transition zone metabauxites. At higher M2 grades this foliation is overgrown by corundum, increasing in grain size with M2 grade.

4.2. Marble pockets included in emeries

Small pockets of coarse-grained, granular calcite marbles, which can easily be disaggregrated by hand, are locally included in the emeries. In thin section the marbles show a very well-equilibrated foam texture (Fig. 7) characterized by equiaxed grains, with almost all grain boundaries meeting at 120° triple junctions. These are the classic textures found in many materials, associated with surface energy-driven normal grain growth.

In contrast, most high-grade marbles outside the emeries have microstructures typical for high-temperature dynamic recrystallization, such as lobate grain boundaries, large subgrains and orientation families (Fig. 8, cf. Urai et al., 1986), indicating grain growth during deformation (cf. Covey-Crump and Rutter, 1989).

5. Discussion

Although the surrounding marbles are isoclinally folded, the diasporite boudins show little evidence of internal deformation. This indicates that during the long and undoubtedly complicated history of diagenesis and M1 + M2-metamorphism, diasporites were sufficiently stronger than the surrounding marbles to remain essentially undeformed during periods of marble deformation. Because the Naxos metabauxites of zone I contain 50–80% diaspore, large amounts of water must be released during the diasporite–corundite transformation. In addition there is a substantial decrease in solid volume (creation of porosity) of the metabauxite lens. Geochemical and petrographical data (Feenstra, 1985) indicate that 6–8 wt% H_2O (equivalent to 40–50% rock volume at the P–T of the phase transition) needs to be expelled and that the phase transformation is accompanied by a solid volume decrease of at least 20% in an average metabauxite lens.

Table 1
Summary of the microstructural observations made in this study

Zone	Sample	Latitude	Longitude	Deformed pisoids	Veins	FOL[b]	Porphyroblasts
I	AFN27	36°57′40″	25°33′05″		X		
I	AFN28	36°57′40″	25°33′05″				
I	AF122B	36°58′55″	25°32′50″		X		
I	AF121A	36°58′55″	25°33′05″		X		
I	AF32C	36°35′25″	25°28′00″	Some	X	X	Chloritoid over diaspore
I	AF55	37°01′45″	25°33′45″				
I	AF58	37°01′45″	25°33′45″				
I/II	40AF71	36°58′20″	25°28′35″	X		X	Corundum over foliation
I/II	AFN34	36°58′40″	25°28′45″	X	X		
II	BN11A	37°00′10″	25°29′30″	X			Corundum over pisoids
III	AFN36	37°02′35″	25°30′00″	X		X	Corundum over foliation
III	AFN37	37°02′35″	25°30′00″	X		X	Corundum over foliation
III	NO4C	37°02′34″	25°30′00″	X		X	Corundum over foliation
III	NO4D	37°02′34″	25°30′00″	X		W	Corundum
III	S262	37°00′10″	25°24′25″	X	late	X	Corundum over foliation
IV	AF147	37°01′30″	25°27′50″	X		X	Corundum over pisoids
IV	AF131B	37°04′50″	25°31′05″	X		X	Corundum over foliation
IV	AFN35	37°04′50″	25°31′05″	X			Corundum over pisoids
IV	AFN39	37°04′50″	25°31′05″	X		X	Corundum over pisoids
IV	AF106-2	37°07′45″	25°34′00″	X		X	Corundum +White mica over foliation
IV	AF106-5	37°07′45″	25°34′00″	X			Kyanite over pisoids
IV	N050[a]	37°07′20″	25°33′40″	X		X	Corundum over foliation
IV	N05A[a]	37°07′20″	25°33′40″	X		X	Corundum over foliation
IV	N05B[a]	37°07′20″	25°33′40″	X		X	Corundum over foliation
IV	N05E[a]	37°07′20″	25°33′40″	X		X	Corundum over foliation
IV	N05F[a]	37°07′20″	25°33′40″	X		X	Corundum over foliation
IV	N05G[a]	37°07′20″	25°33′40″	X		X	Corundum over foliation
IV	N05H[a]	37°07′20″	25°33′40″	X		X	Corundum over foliation
IV	N05I[a]	37°07′20″	25°33′40″	X		W	Corundum +Tourmaline
IV	N05K[a]	37°07′20″	25°33′40″	X		W	Corundum
IV	N05L[a]	37°07′20″	25°33′40″	X			
IV/V	AF104A	37°11′40″	25°32′35″	X		X	Corundum
IV/V	AF104B	37°11′40″	25°32′35″	X		X	Corundum over foliation
IV/V	BN42	37°11′40″	25°32′35″	X		X	Corundum over foliation
IV/V	AF143D	37°11′40″	25°32′35″	X		X	Corundum over foliation

[b] FOL = foliation: X = yes or present; W = weak foliation.
[a] N050–N05L were collected along a 6.2 m long profile from rim (O) to centre (L) of an ~10 m diameter emery deposit.

Because the emeries (predominantly polycrystalline α-Al_2O_3) are much stronger than marbles under the conditions involved, the presence of strong internal deformation in the emeries appears puzzling. It can be explained, however, by a transient weakening accompanying the diasporite–corundite dehydration. The assumptions we need to make are as follows.

1. Before M2, the emeries had the same pisoid morphologies as now seen in the diasporites. This is reasonable because the corundum-in isograd cuts across the lithological layering; emeries and diasporites probably are stratigraphically equivalent. In addition, strongly deformed diasporites enclosed in marbles have not yet been observed (G. Bardossy, personal communication 1998).
2. During dehydration of the diasporites the surrounding marbles were deforming. As argued by Urai et al. (1991), there was a major deformation phase during M2, involving most units in the metamorphic complex upgrade of the biotite-in isograd. Microstructures in the high-grade marbles indicate high-temperature deformation. Although no detailed information is available on the exact distribution of strain in space and time, there is ample evidence for a major phase of deformation during M2.
3. During transformation the dewatering metabauxite mass had mechanical properties which were comparable to or weaker than the surrounding marbles, of which the mechanical properties can be estimated based on extrapolation of experimental data (Schmid et al., 1980). The low strength then allows part of the strain in the surrounding marbles to be taken up by the emeries.

Based on these assumptions, we infer the processes in the metabauxites during M2 as follows.

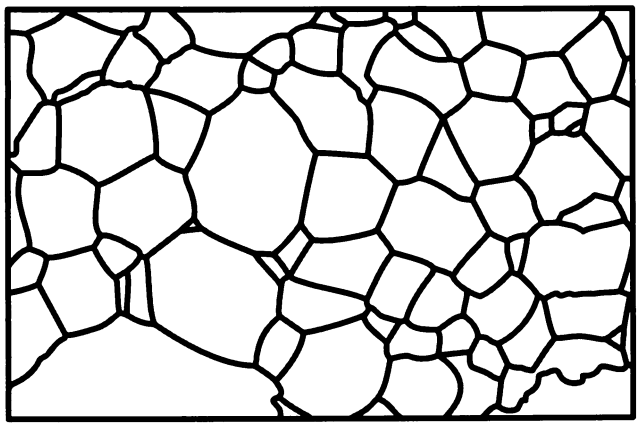

Fig. 7. Microstructure (tracing of grain boundaries in a photomicrograph) of marble inclusion in emery from zone IV, showing classic static grain growth microstructure. Width of photo is 25 mm.

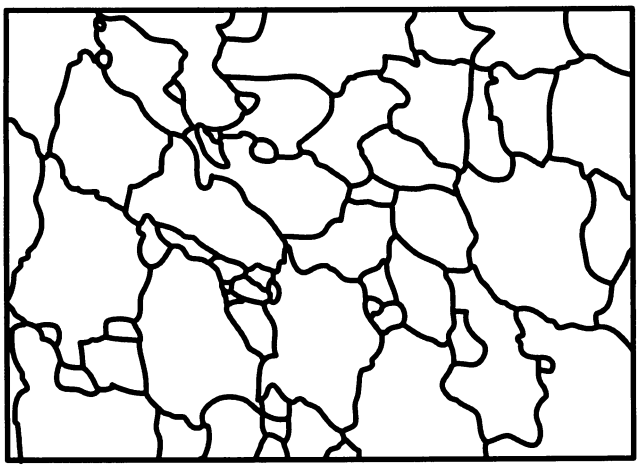

Fig. 8. Microstructure (tracing of grain boundaries in a photomicrograph) of marble outside the emeries from zone IV, showing the coarse-grained microstucture typical of dynamic recrystallization. Width of photo is 25 mm.

Owing to the initial low permeability, both in metabauxite and surrounding marbles, and the large H_2O-buffer capacity of diaspore, prograde reaction has rapidly generated water pressures close to the minimum principal stress σ_3 in the metabauxites (cf. Wong et al., 1997). The occurrence of the first corundum in the outer parts of the deposits as well as the presence of veinlets with inclusion-free corundum, indicates that the initial permeability of the diasporites was low. The corundum veinlets are interpreted to represent tensile fractures ($P_{\text{fluid}} = \sigma_3$) that allowed the dehydration water to escape from the metabauxite lens, during the early stages of transformation when the reacting mass was still cohesive.

At a later stage, deformation in the reacting metabauxites became much more pervasive, producing the macroscopically ductile structures described above. The deformation mechanism in the dehydrating metabauxite is interpreted to have involved some kind of grain-sliding process, assisted by loss of cohesion between grains in the reacting diaspore–corundum mixture. Due to the processes described in the introduction, a fine-grained emery in which a $P_{\text{fluid}} = \sigma_3$ is maintained can be as weak or weaker than the surrounding deforming marbles, and part of the total strain during this period was taken up by the metabauxites. In this context, it is noted that the weakening of the dehydrating diasporites must have been more than that of the surrounding marbles owing to the temperature increase during M2 (differential stresses decreasing from 50 to 5 MPa as suggested by the recrystallized grain size).

During the dehydration reaction the permeability of the reacting mass has probably increased dramatically, and the high fluid pressures were contained by the low permeability marbles surrounding the compacting metabauxites. After the reaction was nearly complete, pore pressure decreased to values less than σ_3, the corundum aggregate started compacting and quickly became cohesive and stronger than the surrounding marbles. At this point deformation in the metabauxites stopped, while the surrounding marbles probably continued deforming.

The rate of compaction of the corundum aggregate and the porosity at which it becomes stronger than the surrounding marbles is difficult to estimate. Although there is an extensive literature on the sintering of alumina (Bruch, 1962; Coble, 1962; Nichols, 1966; Kellett and Lange, 1988; Yeh and Sacks, 1988), the available data were obtained at much higher temperatures and strain rates, and extrapolation to the conditions of this study is very difficult.

During the rest of M2, the emeries were equilibrated under essentially static conditions. This is shown by the microstructures in the marble pockets inside the emeries, which show classic examples of thermally activated static grain growth. Static high-T equilibration is also indicated by corundum porphyroblasts overgrowing the foliation formed by flattened pisoids as well as the typical post-tectonic growth of amphibolite-facies M2 minerals.

The diaspore–corundum reaction is estimated to take place at ~420–450°C on Naxos, while the highest-grade emeries that still display relict pisoidic textures reached ~620°C under peak conditions. The microstructures thus provide evidence that deformation began during the prograde, heating-up stage of M2. In general, very little information is preserved from this early stage in the metamorphic history of rocks.

The rate of a prograde metamorphic reaction depends on a number of factors, such as heat and mass transport towards and away from the site of mineral growth, surface reaction mechanisms, dissolution of reactants and nucleation and growth of products. The slowest of these processes will control the reaction rate (e.g. Walther and Wood, 1984; Lasaga, 1986). Compared with more common prograde metamorphic reactions (e.g. in pelitic rocks), little mass transport is required for the diaspore–corundum reaction.

The most important rate-controlling factor may in fact be the escape of the generated water from the reacting site, since high P_{H_2O} will stabilize diaspore.

Kinetic data on the dissolution of diaspore and nucleation and growth of corundum at the P–T conditions of the Naxos isograd are unavailable. Hydrothermal experimental investigations (e.g. Haas, 1972; Fockenberg et al., 1996) of the diaspore–corundum equilibrium suggest, however, that the kinetics of the reaction is rather fast. Furthermore, epitaxial relationships between diaspore and corundum as found in samples of the transition zone (Feenstra, 1985) will facilitate reaction. It is argued therefore that dissolution of diaspore and nucleation and growth of corundum are not limiting the reaction rate, but that the dominating rate-controlling factor may be the escape of the dehydration water.

Another rate-controlling factor that should be considered is the rate of heat supply to the reaction site. This may result in buffering of temperature by the reaction (see e.g. Rice and Ferry, 1982; Ridley, 1986). The diaspore–corundum reaction is strongly endothermic and as diaspore is the main mineral in the rock an amount of heat of circa 1.2 kJ/cm^3 is required to complete the diasporite–corundite transformation.

In conclusion, we presented a natural example of dehydration producing transient weakening of metabauxites. There are not many natural examples of this phenomenon known from experiments, and it is thought to be important during prograde regional metamorphism.

Acknowledgements

JLU wishes to thank Paul Williams for guidance, support, friendship and a lot of fun during the past twenty or so years. We thank Olaf Schuiling, Ben Jansen, Gordon Lister and Dave Olgaard for illuminating discussions on Naxos geology and on the mechanical properties of dehydrating rocks. Discussions with Michael Sax on the deformation of alumina and comments by Kate Brodie and John Ridley on an early version of the manuscript are gratefully acknowledged. Constructive review by Dave Olgaard is gratefully acknowledged. Financial support to JLU by a C&C Huygens fellowship of NWO is gratefully acknowledged. The latter organization also financially supported the Ph.D. research of AF.

References

Andriessen, P.A.M., 1991. K–Ar and Rb–Sr age determinations on micas of impure marbles on Naxos, Greece: the influence of metamorphic fluids and lithology on the blocking temperature. Schweizerische Mineralogische und Petrographische Mitteilungen 71, 89–99.

Andriessen, P.A.M., Banga, G., Hebeda, E.H., 1987. Isotopic age study of pre-Alpine rocks in the basal units on Naxos, Sikinos and Ios, Greek Cyclades. Geologie en Mijnbouw 66, 3–14.

Baker, J., Matthews, A., 1995. The stable isotopic evolution of a metamorphic complex, Naxos, Greece. Contrib. Mineral. Petrol. 120, 391–403.

Bardossy, G., 1982. Karstbauxites: Bauxite Deposits on Carbonate Rocks. Developments in Economic Geology, 14. Elsevier, Amsterdam, p. 441.

Bonneau, M., Geyssant, J., Lepvrier, C., 1978. Tectonique alpine dans le massif d'Attique–Cyclades (Grèce): Plis couchés kilometriques dans l'Île de Naxos, consequences. Rev de Geophys et de Géol dyn (2) XX (1), 109–122.

Boronkay, K., Doutsos, T., 1994. Transpression and transtension within different structural levels in the central Aegean region. Journal of Structural Geology 16, 1555–1573.

Bruch, C.A., 1962. Sintering kinetics for the high density alumina process. Ceramic Bulletin 41 (12), 799–806.

Buick, I.S., 1991a. The late Alpine evolution of an extensional shear zone. Naxos, Greece. Journal of the Geological Society 148, 93–103.

Buick, I., 1991b. Mylonite fabric development on Naxos, Greece. Journal of Structural Geology 13, 643–655.

Buick, I.S., Holland, T.J.B., 1989. The P–T path associated with crustal extension, Naxos, Cyclades, Greece. In: Daly, J.S., Cliff, R.A., Yardley, B.W.D. (Eds.). Evolution of Metamorphic Belts. Geological Society of London Special Publication, 43. Geological Society, London, pp. 365–369.

Coble, R.L., 1962. Sintering Alumina: effect of atmospheres. Journal of the American Ceramic Society 45 (3), 123–128.

Covey-Crump, S.J., Rutter, E.H., 1989. Thermally-induced grain growth of calcite marbles on Naxos Island, Greece. Contributions to Mineralogy and Petrology 101, 69–86.

Feenstra, A. (1985) Metamorphism of bauxites on Naxos, Greece. PhD Thesis, University of Utrecht, Geologica Ultraiectina 39, 206 pp.

Feenstra, A., 1996. An EMP and TEM–AEM study of margarite, muscovite, paragonite in polymetamorphic metabauxites rocks of Naxos (Cyclades, Greece) and the implications of fine-scale mica interlayering and multiple mica generations. Journal of Petrology 37, 201–233.

Fockenberg, T., Wunder, B., Grevel, K.-D., Burchard, M., 1996. The equilibrium diaspore–corundum at high pressure. European Journal of Mineralogy 8, 1293–1299.

Gautier, P., Brun, J.P., 1994. Ductile crust exhumation and extensional detachment in the central Aegean (Cyclades and Evvia islands). Geodynamica Acta 7, 57–85.

Gautier, P., Brun, J.P., Jolivet, L., 1993. Structure and kinematics of upper Cenozoic extensional detachment on Naxos and Paros (Cyclades islands, Greece). Tectonics 12, 1180–1194.

Haas, H., 1972. Diaspore–corundum equilibrium determined by epitaxis of diaspore on corundum. American Mineralogist 57, 1375–1385.

Heard, H.C., Rubey, W.W., 1966. Tectonic implications of gypsum dehydration. Geological Society of America Bulletin 77, 741–760.

Hecht, J., 1979. Geologische Karte des Schmirgel-führenden Gebietes zwischen Apiranthos und Koronos, Naxos, Griechenland; 1:10000. Institute of Geology and Mining Research (IGME), Athens.

Jansen, J.B.H., Schuiling, R.D., 1976. Metamorphism on Naxos: petrology and geothermal gradients. American Journal of Science 276, 1225–1253.

John, B.E., Howard, K.A., 1995. Rapid extension recorded by the cooling-age patterns and brittle deformation, Naxos, Greece. Journal of Geophysical Research 100, 9969–9979.

Kellett, B.J., Lange, F.F., 1988. Experiments on pore closure during hot isostatic pressing and forging. Journal of the American Ceramic Society 71 (1), 7–12.

Ko, S.-c., Olgaard, D.L., Briegel, U., 1995. The transition from weakening to strengthening in dehydrating gypsum: evolution of excess pore pressures. Geophysical Research Letters 22, 1009–1012.

Ko, S.-c., Olgaard, D.L., Wong, T.-f., 1997. Generation and maintenance of pore pressure excess in a dehydrating system: 1. Experimental and microstructural observations. Journal of Geophysical Research 102 (B1), 825–839.

Lasaga, A.C., 1986. Metamorphic reaction rate laws and development of isograds. Mineralogical Magazine 50, 359–373.

Lewis, S., Holness, M., Graham, C., 1998. Ion microprobe study of marble from Naxos, Greece; grain-scale fluid pathways and stable isotope equilibration during metamorphism. Geology 26, 935–938.

Lister, G.S., Banga, G., Feenstra, A., 1984. Metamorphic core complexes of Cordilleran type in the Cyclades, Aegean Sea, Greece. Geology 12, 221–225.

Lister, G.S., Baldwin, S.L., 1993. Plutonism and the origin of metamorphic core complexes. Geology 21, 607–610.

Lister, G.S., Forster, M. (Eds.), 1998. Inside the Aegean Metamorphic Core Complexes: a Field Trip Guide Illustrating the Geology of the Aegean Metamorphic Core Complexes Australian Crustal Research Centre, Technical Publication, 45. Monash University, Melbourne.

Morris, A., Anderson, M., 1996. First palaeomagnetic results from the Cycladic Massif, Greece, and their implications for Miocene extension directions and tectonic models in the Aegean. Earth and Planetary Science Letters 142, 397–408.

Newman, J., Lamb, W.M., Drury, M.R., Vissers, R.L.M., 1999. Reaction-softening by an H_2O deficient, continuous net transfer reaction. Tectonophysics 303, 193–222.

Nichols, F.A., 1966. Theory of grain growth in porous compacts. Journal of Applied Physics 37 (13), 4599–4602.

Okrusch, M., Bröcker, M., 1990. Eclogites associated with high-grade blueschists in the Cyclades archipelago, Greece: a review. Eur. J. Mineral. 2, 451–478.

Olgaard, D.L., Ko, S.-c., Wong, T.-f., 1994. Deformation and pore pressure in dehydrating gypsum under transiently drained conditions. Tectonophysics 245, 237–248.

Paterson, M.S., Luan, F.C., 1990. Quartzite rheology under geological conditions. In: Knipe, R.J., Rutter, E.H. (Eds.). Deformation Mechanisms, Rheology and Tectonics. Geological Society, London, pp. 299–307.

Pe-Piper, G., Kotopouli, C.N., Piper, D.J.W., 1997. Granitoid rocks of Naxos, Greece; regional geology and petrology. Geological Journal 32, 153–171.

Raleigh, C.B., Paterson, M.S., 1965. Experimental deformation of serpentinite and its tectonic implications. Journal of Geophysical Research 70, 3965–3985.

Rice, J.M., Ferry, J.M., 1982. Buffering, infiltration, and the control of intensive variables during metamorphism. In: Ferry, J.M. (Ed.). Characterization of Metamorphism through Mineral Equilibria. Reviews in Mineralogy, 10. Mineral Society of America, Washington, DC, pp. 263–326.

Ridley, J., 1982. Arcuate lineation trends in a deep level, ductile thrust belt, Syros, Greece. Tectonophysics 88, 347–360.

Ridley, J., 1986. Modelling of the relations between reaction enthalpy and the buffering of reaction progress in metamorphism. Mineralogical Magazine 50, 375–384.

Rutter, E.H., Brodie, K.H., 1988. Experimental 'syntectonic' dehydration of serpentinite under conditions of controlled water pressure. Journal of Geophysical Research 93 (B5), 4907–4932.

Schmid, S.M., Paterson, M.S., Boland, J.N., 1980. High temperature flow and dynamic recrystallization in Carrara marble. Tectonophysics 65, 245–280.

Spakman, W., Wortel, M.J.R., Vlaar, N.J., 1988. The Hellinic subduction zone: a tomographic image and its geodynamic implications. Geophysical Research Letters 15, 60–63.

Urai, J.L., Means, W.D.M., Lister, G.S., 1986. Dynamic Recrystallization of Minerals. American Geophysical Union, Geophysical Monograph (the Paterson volume), 36. American Geophysical Union, Washington, DC, pp. 161–199.

Urai, J.L., Schuiling, R.D., Jansen, J.B.H., 1991. Alpine deformation on Naxos (Greece). In: Knipe, R.J., Rutter, E.H. (Eds.). Deformation Mechanisms, Rheology and Tectonics. Geological Society Special Publication, 54. Geological Society, London, pp. 509–522.

Walther, J.V., Wood, B.J., 1984. Rate and mechanism in prograde metamorphism. Contrib. Mineral. Petrol. 88, 246–259.

Wong, T.-f., Ko, S.-c., Olgaard, D.L., 1997. Generation and maintenance of pore pressure excess in a dehydrating system: 2. Theoretical analysis. Journal of Geophysical Research 102 (B1), 841–852.

Wybrans, J.R., McDougall, I., 1988. Metamorphic evolution of the Attic Cycladic Metamorphic Belt on Naxos (Cyclades, Greece) utilizing $^{40}Ar/^{39}Ar$ age spectrum measurements. Journal Metamorphic Geology 6, 571–594.

Yeh, T.-S., Sacks, M.D., 1988. Low-temperature sintering of aluminium oxide. Journal of the American Ceramic Society 71 (10), 841–844.